^{18}F-Fluorocholine PET/CT Is More Sensitive Than ^{11}C-Methionine PET/CT for the Localization of Hyperfunctioning Parathyroid Tissue in Primary Hyperparathyroidism

Céline Mathey[1], Caroline Keyzer[2], Didier Blocklet[1], Gaetan Van Simaeys[1], Nicola Trotta[1], Simon Lacroix[1], Bernard Corvilain[3], Serge Goldman[1], and Rodrigo Moreno-Reyes[1]

[1]Department of Nuclear Medicine and PET/Biomedical Cyclotron Unit, Hôpital Érasme, Université Libre de Bruxelles, Brussels, Belgium; [2]Department of Medical Imaging, Hôpital Erasme, Université Libre de Bruxelles, Brussels, Belgium; and [3]Department of Endocrinology, Hôpital Érasme, Université Libre de Bruxelles, Brussels, Belgium

Preoperative molecular imaging is paramount to direct surgery in primary hyperparathyroidism (pHPT). We investigated the diagnostic performance of ^{18}F-fluorocholine (^{18}F-FCH) PET/CT compared with ^{11}C-methionine (^{11}C-MET) PET/CT for localization of hyperfunctioning parathyroid tissue in patients with pHPT and negative or inconclusive ^{99m}Tc-sestaMIBI (^{99m}Tc-MIBI) SPECT findings. **Methods:** Fifty-eight patients with biochemical evidence of pHPT and negative or inconclusive ^{99m}Tc-MIBI SPECT findings were referred for presurgical detection and localization of hyperfunctioning parathyroid tissue by ^{11}C-MET and ^{18}F-FCH PET/CT. The PET/CT results were classified into 3 categories (positive, inconclusive, or negative) based on the nodular aspect of tracer uptake and the visualization of corresponding nodules on CT. The PET/CT results were correlated with the surgical and histopathologic findings, which were used as the gold standard. **Results:** Fifty-three patients were included for analysis. ^{18}F-FCH PET/CT was positive in 39 patients (74%), inconclusive in 5 (9%), and negative in 9 (17%), compared with 25 (47%), 12 (23%), and 16 (30%), respectively, for ^{11}C-MET PET/CT. ^{18}F-FCH localized 11 additional foci (6 positive and 5 inconclusive), compared with ^{11}C-MET. Twenty-six patients (sex ratio, 10/16 M/F) underwent surgery, with resection of 31 lesions (22 adenomas, 6 hyperplastic glands, and 3 carcinomas) and 1 normal gland. At follow-up, 21 patients (81%) were considered cured after surgery, whereas 3 patients (12%) had persistence of hypercalcemia. With inconclusive cases being considered negative, ^{18}F-FCH PET/CT correctly localized 26 lesions in 24 of 26 patients (92%), compared with 16 lesions in 15 of 26 patients (58%) localized by ^{11}C-MET PET/CT. Per-patient–based sensitivity and positive predictive value were 96% and 96%, respectively, for ^{18}F-FCH and 60% and 94%, respectively, for ^{11}C-MET ($P <$ 0.0001). Per-lesion–based sensitivity and positive predictive value were 84% and 90%, respectively, for ^{18}F-FCH and 52% and 94%, respectively, for ^{11}C-MET ($P <$ 0.0001). **Conclusion:** In the presence of biochemical evidence of pHPT with negative or inconclusive ^{99m}Tc-MIBI SPECT findings, ^{18}F-FCH PET/CT performs better than ^{11}C-MET PET/CT for the detection of pathologic parathyroid tissue, allowing localization of parathyroid adenoma or hyperplasia in 96% of patients.

Key Words: primary hyperparathyroidism; parathyroid adenoma; ^{18}F-fluorocholine; ^{11}C-methionine; PET/CT

Primary hyperparathyroidism (pHPT) is one of the most frequent endocrine disorders, with a prevalence of about 2% in women older than 50 y. Long-term consequences of pHPT affect mainly the skeleton (osteoporosis, fractures) and the kidney (nephrolithiasis, impaired renal function). Diagnosis is based on increased serum calcium, low phosphorus levels, and inappropriate parathyroid hormone (PTH) levels (1). pHPT is associated with a solitary parathyroid adenoma (PA) in 80%–90% of patients or, more rarely, multiglandular disease or diffuse parathyroid hyperplasia (1).

Optimal management of pHPT consists of preoperative localization of the abnormal parathyroid gland, allowing for minimally invasive parathyroidectomy (2,3). Conventional first-line presurgical imaging is based on ^{99m}Tc-sestaMIBI (^{99m}Tc-MIBI) parathyroid scintigraphy with subtraction images, usually complemented by ultrasonography. It ideally includes a SPECT/CT acquisition, with a detection rate of 84%–88% (4,5).

Currently, in cases of negative or equivocal scintigraphy results, results discrepant with ultrasonography, or persistence or recurrence of HPT after surgery, an alternative investigation is recommended involving hybrid PET/CT technique, usually with an amino acid tracer such as ^{11}C-methionine (^{11}C-MET) (6,7). Use of PET/CT for that purpose offers a shorter acquisition time and higher spatial resolution and sensitivity (8). Metaanalyses reported ^{11}C-MET to have sensitivity of 77%–81% in a per-patient–based analysis in patients with pHPT and negative or inconclusive ^{99m}Tc-MIBI SPECT findings (6,9). However, the short half-life of ^{11}C-MET imposes on-site production and strict acquisition conditions (6).

More recently, ^{18}F-fluorocholine (^{18}F-FCH) PET/CT used for imaging prostatic neoplasia assessment (10) has been shown capable of localizing an abnormal parathyroid gland in patients with negative or inconclusive ^{99m}Tc-MIBI SPECT results (3,8,11,12). It has the advantages over ^{11}C-MET of a longer half-time and a more favorable positron energy. Choline is a precursor of phospholipids, which are essential constituents of cellular lipidic structures. ^{18}F-FCH is therefore a tracer of lipid metabolism whose uptake increases after increased intracellular metabolism requiring synthesis of phospholipids.

The aim of this study was to investigate whether, in patients with pHPT and negative or inconclusive ^{99m}Tc-MIBI SPECT results, the diagnostic performance of ^{18}F-FCH PET/CT is similar to that of ^{11}C-MET PET/CT from a preoperative perspective. The secondary objective was to compare the performance of the 2 methods in the detection of individual hyperfunctioning parathyroid lesions.

MATERIALS AND METHODS

Patients

Between November 2015 and December 2018, we prospectively included 58 patients with biologically proven pHPT (hypercalcemia and elevated or inappropriately normal PTH levels) and negative or inconclusive results on ^{99m}Tc-MIBI imaging performed at various institutions, including ours, and involving SPECT with or without combined CT.

On inclusion, and when there was no recent blood test (<3 mo) confirming hyperparathyroidism, a blood sample was taken to measure serum values of calcium, phosphorus, PTH, albumin, and vitamin D. The serum calcium level was measured the day after surgery to check for normalization.

Institutional ethics committee approval was obtained before the start of this prospective study, and all subjects signed an informed-consent form (P2015/307).

PET/CT Procedure

All PET/CT was performed on a Gemini GXL ($n = 15$) or a TF64 ($n = 38$) PET/CT camera (Philips), with essentially identical protocols on both systems. All patients sequentially underwent ^{11}C-MET and ^{18}F-FCH PET/CT (Supplemental Fig. 1; supplemental materials are available at http://jnm.snmjournals.org).

[11]C-MET PET/CT. All patients were injected with an average bolus of 555 MBq of ^{11}C-MET while in a fasting state. Fifteen minutes after injection, unenhanced CT (40 mAs; 120 kV; slice thickness, 2.0 mm; interval, 1.5 mm) was performed, followed by a PET acquisition of the neck and upper mediastinum (3 bed positions, 7 min per bed position). Images were reconstructed with 2 different algorithms depending on the PET camera (blob-basis function ordered-subsets time of flight or line-of-response–based row-action maximum likelihood).

^{18}F-FCH PET/CT. Approximately 3 h after ^{11}C-MET injection, unenhanced CT (40 mAs; 120 kV; slice thickness, 2.0 mm; interval, 1.5 mm) was acquired. Then, with the patient lying in the PET/CT tomograph, a 4-MBq dose of ^{18}F-FCH per kilogram of body mass was administered intravenously. ^{18}F-FCH was prepared in 2 steps using a fully automated radiochemistry synthesizer (Trasis All-in-One) (*13*). A 15-min dynamic PET acquisition covering the neck was started at the time of tracer injection, followed by a static acquisition (early ^{18}F-FCH [^{18}F-FCH$_E$]) on the neck and the upper mediastinum (3 bed positions, 7 min per bed position). PET/CT imaging of the neck and upper mediastinum was repeated 60 min after injection (late ^{18}F-FCH [^{18}F-FCH$_L$]) and used for image analysis in the present work. Images were reconstructed with 2 different algorithms depending on the PET camera (blob-basis function ordered-subsets time of flight or line-of-response–based row-action-maximum likelihood).

Image Interpretation. All PET/CT images were analyzed independently by a nuclear medicine physician (11 y of experience) and a radiologist (18 y of experience), who were aware of previous imaging and laboratory findings for the patients, and by a nuclear medicine physician (27 y of experience) masked to any clinical and imaging information. Discordant image interpretation occurred in 11 patients. In all these cases, a consensus reading led to a final common interpretation. There was no pause between ^{18}F-FCH and ^{11}C-MET readings.

The images (maximum-intensity projection and 3-dimensional volume) were evaluated visually to determine the number and exact location of uptake areas suggestive of hyperfunctioning parathyroid glands.

The results were classified into 3 categories based on the aspect of the tracer uptake area and the visualization of corresponding nodules on CT: positive, in cases of a clear circumscribed uptake area on PET images or a faint circumscribed uptake area corresponding to a nodular lesion on CT; inconclusive, in cases of a faint uptake area with no corresponding nodule on CT; or negative, in cases of no discernable tracer uptake area. Lesion localization was assigned to 6 anatomic regions: right and left upper, right and left lower, intrathyroidal, and ectopic. In cases of a discrepancy between readers' assessments, the appropriate category and anatomic localization were assigned by consensus.

The semiquantitative analysis was performed with Philips IntelliSpace Portal software (version 9). The SUV$_{max}$ and SUV$_{mean}$ of the PA were measured. We estimated the contrast between the lesion and the thyroid using the ratio of PA SUV$_{max}$ to thyroid SUV$_{mean}$ (PA/thyroid). By this ratio, we evaluated the capacity to identify the parathyroid activity close to the organ it usually lies behind. The SUV$_{max}$ and SUV$_{mean}$ of the thyroid were measured by placing a spheric volume of interest 1 cm^3 in diameter on the contralateral thyroid lobe unless morphologically pathologic or the right lobe in the absence of a lesion.

Surgery and Histology

Surgeons were aware of ^{11}C-MET and ^{18}F-FCH PET/CT data for all patients. They used this information to direct the surgical procedure, which was an open, minimally invasive parathyroidectomy in cases of a single area of uptake on ^{11}C-MET or ^{18}F-FCH PET/CT. If multiple lesions or an ectopic location were suspected, the surgical approach was adapted. In cases of a coexisting multinodular goiter or suggestive thyroid nodules, an additional hemithyroidectomy or total thyroidectomy was performed. All operated cases had at least 1 lesion categorized as positive on either the ^{11}C-MET or the ^{18}F-FCH PET/CT, except for 1 patient with negative results on PET/CT, for whom full surgical exploration was decided for recurrent pHPT.

The results of ^{11}C-MET and ^{18}F-FCH PET/CT were compared with the surgical exploration and histopathologic findings. Surgical success was established according to normalization of postoperative serum calcium level.

Statistical Analysis

Quantitative variables are expressed as mean ± SD for normally distributed continuous variables and as median with 25th and 75th percentiles for nonnormal continuous variables.

For the sake of comparison, negative, inconclusive, and positive lesions were scored 0, 1, and 2, respectively. Tracer comparison of visual scoring performance was evaluated with a Wilcoxon matched-pairs signed-rank test. For visual decision performance on matched pairs of ^{11}C-MET and ^{18}F-FCH PET/CT images, inconclusive results were considered negative, and the McNemar test with the continuity correction was used.

The sensitivity and positive predictive value of PET/CT imaging were evaluated on a per-lesion and per-patient basis and calculated using histology analysis as the gold standard. Since no histologic data were available in most patients with negative results on PET/CT, specificity and negative predictive values were not evaluated.

The D'Agostino and Pearson test and the Shapiro–Wilk test were used to assess the normality of the sample values. Repeated measures of each relevant quantitative parameter (SUV$_{max}$ PA and PA/thyroid) were analyzed with the Friedman test. Dunn tests were subsequently applied for multiple comparisons between tracers (^{11}C-MET, ^{18}F-FCH$_E$, and ^{18}F-FCH$_L$). Nonparametric Spearman correlation r was calculated between ^{18}F-FCH$_E$ and ^{18}F-FCH$_L$ PET/CT with respect to ^{11}C-MET images for PA/thyroid. After exclusion of negative cases, simple linear regression was further calculated to evaluate how this quantitative parameter varies in ^{18}F-FCH$_E$ and ^{18}F-FCH$_L$ PET/CT with respect to the corresponding

parameter on ^{11}C-MET images. Runs tests were performed to assess lack of fit. Goodness of fit was assessed with R^2. Statistical analyses were performed using Prism, version 9.0 (GraphPad Software), and its online McNemar test calculator. For all tests, a P value of less than 0.05 was considered statistically significant.

RESULTS

Among 58 patients who prospectively underwent ^{11}C-MET and ^{18}F-FCH PET/CT, 53 patients were included in the analysis (Fig. 1). Five patients were excluded because of unconfirmed pHPT ($n = 4$) or technical problems ($n = 1$). The characteristics of the 53 patients are summarized in Table 1. Among them, 7 had a previous history of parathyroidectomy and persistent or recurrent pHPT. Four patients with familial pHPT were included, 3 of whom had previous surgery. Participants underwent ^{11}C-MET and ^{18}F-FCH PET/CT on the same day, except for 7 patients who underwent their 2 PET/CT scan within 5 mo. Twenty-six patients (16 women and 10 men) had parathyroidectomy, with histopathologic confirmation of the presence of adenoma or hyperplasia in 24 patients. Fourteen patients had negative (9/53) or inconclusive (5/53) PET/CT results. Goiter was present in 10 patients (19%), and 29 patients had nodular thyroid disease (55%).

^{18}F-FCH PET/CT Outperforms ^{11}C-MET PET/CT for Lesion Localization at Both Early and Late Time Points in the Prospect of Surgery Guidance

^{18}F-FCH PET/CT was positive in 39 patients (74%) and inconclusive in 5 patients (9%), compared with 25 patients (47%) and 12 patients (23%), respectively, for ^{11}C-MET PET/CT (Table 2). The visual scoring performance of ^{18}F-FCH PET/CT was greatly superior to that of ^{11}C-MET PET/CT on a per-patient basis (Wilcoxon $P < 0.0001$). Also, the McNemar test of matched-pairs discordant results also demonstrated the superiority of ^{18}F-FCH over ^{11}C-MET PET/CT in visual decision performance on a per-patient basis ($P = 0.0005$; $\chi^2 = 12.071$ with $1°$ of freedom), with 14 patients positive only with ^{18}F-FCH PET/CT and no patient positive only with ^{11}C-MET PET/CT, whereas 25 patients were positive and 14 were negative with both tracers. Of 26 patients with negative or inconclusive ^{99m}Tc-MIBI results and positive PET/CT results (either ^{11}C-MET or ^{18}F-FCH) who had surgery, 17 were switched from a cervical exploration to a minimally invasive parathyroidectomy approach.

In 24 of 26 (92%) patients who had surgery, hyperfunctioning parathyroid tissue (adenoma/hyperplasia/cancer) was correctly localized with ^{18}F-FCH (26 lesions), compared with 15 patients with ^{11}C-MET (16 lesions). On a per-patient basis, the positive predictive value was 96% for ^{18}F-FCH and 94% for ^{11}C-MET. One patient was negative on both PET/CT scans and underwent a surgical exploration allowing the resection of a PA followed by calcemia normalization. No hyperfunctioning parathyroid tissue was found in a patient with persistent pHPT after surgery. The per-patient sensitivity of ^{18}F-FCH PET/CT was 96%, compared with 60% for ^{11}C-MET PET/CT ($P < 0.0001$). In addition, 5 patients had multiglandular disease detected on ^{18}F-FCH PET/CT (19%). Postoperative calcemia used to define therapeutic success was obtained at 11.5 ± 6.9 mo after surgery. Twenty-one (81%) patients who underwent parathyroidectomy were considered cured, 3 (12%) patients had recurrent or persistent hypercalcemia, and 2 patients were lost to follow-up.

The comparison of lesion visual scoring performance between the 2 tracers is reported in Supplemental Table 1. ^{18}F-FCH PET/CT detected a single uptake area in 37 of 53 patients and multiple uptake areas in 7 of 53 patients. On per-lesion basis (Table 2), ^{18}F-FCH PET/CT showed 47 positive and 9 inconclusive uptake areas. ^{18}F-FCH PET/CT allowed detection of 11 additional uptake areas (6 positive and 5 inconclusive) compared with ^{11}C-MET PET/CT. Thirteen inconclusive uptake areas on ^{11}C-MET were positive on ^{18}F-FCH. Three ectopic parathyroid glands in the superior mediastinum and 2 intrathyroidal localizations were identified with both PET tracers. Comparison of tracers for visual scoring performance on a per-lesion basis revealed the superiority of ^{18}F-FCH over ^{11}C-MET PET/CT (Wilcoxon $P < 0.0001$). Again, the McNemar test revealed, as well, the superiority of ^{18}F-FCH over ^{11}C-MET PET/CT for visual decision performance on a per-lesion basis ($P < 0.0001$; $\chi^2 = 17.053$ with $1°$ of freedom), with 19 lesions positive only with ^{18}F-FCH PET/CT and no lesion positive only with ^{11}C-MET PET/CT, whereas 28 lesions were positive and 18 were negative with both tracers. Except for 2 lesions with rapid washout visualized only on ^{18}F-FCH$_E$, and 1 uncertain lesion found only on ^{18}F-FCH$_L$, all lesions were visualized on early and late acquisitions,
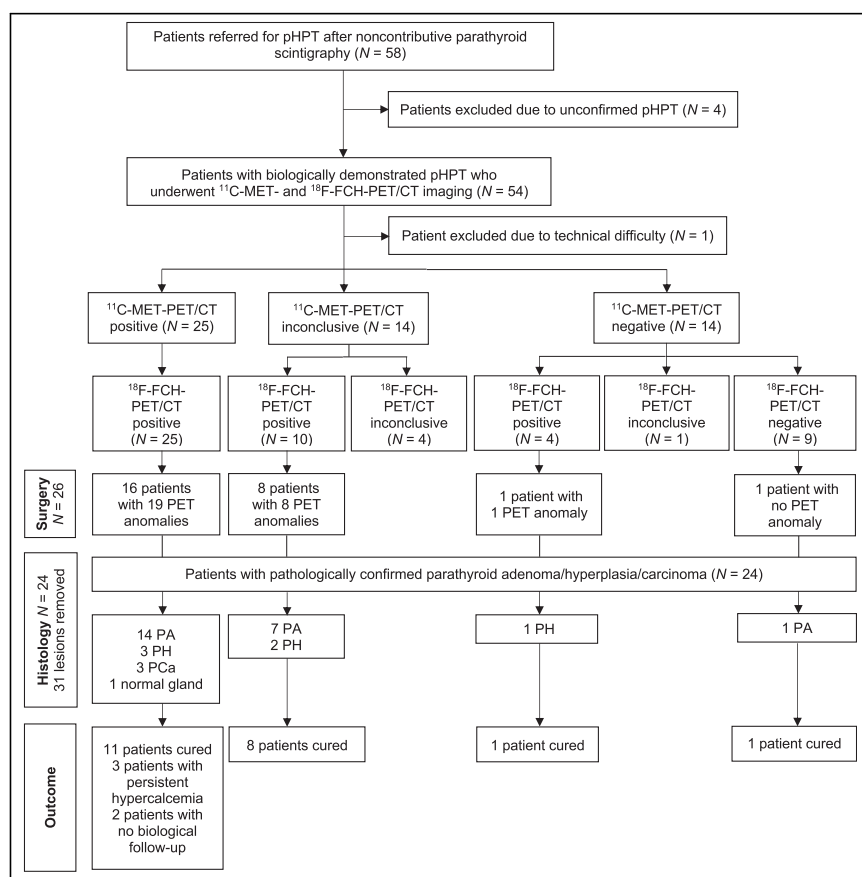

FIGURE 1. Flowchart. PCa = parathyroid carcinoma; PH = parathyroid hyperplasia.

TABLE 1
Patient Characteristics (*n* = 53)

Characteristic	Value	Normal value
Sex (M/F)	16/37	
Age (y)	58 ± 16	
Body mass index (kg/m^2)	28.2 ± 5.5	
Prior parathyroidectomy	7 (13)	
Prior		
^{99m}Tc-MIBI SPECT/CT		
Negative	38 (72)	
Inconclusive	15 (28)	
Ultrasonography	35 (66)	
Other	9 (17)	
Baseline laboratory values		
PTH (ng/L)	72.0 (54–101)	4–49
Calcium (mmol/L)	2.67 (2.62–2.69)	2.12–2.62
Phosphorus (mmol/L)	0.75 ± 0.17	0.81–1.45
25-hydroxycholecalciferol (ng/mL)	24.74 ± 8.97	30–80
^{11}C-MET results		
Positive	25 (47)	
Negative*	28 (53)	
^{18}F-FCH results		
Positive	39 (74)	
Negative*	14 (26)	
Surgical results (*n* = 26)		
Pathologic parathyroid tissue found	24 (92)	
Biologic normalization during follow-up	21 (81)†	

*Negative imaging includes negative or inconclusive results.
†2 patients were lost to follow-up.
Qualitative data are number and percentage; continuous data are mean ± SD; nonnormal continuous data are median and 25th–75th percentiles (D'Agostino–Pearson omnibus test).

without a significant difference in visual scoring assessment of contrast. Two cases are illustrated in Supplemental Figure 2.

In total, 31 glands were surgically removed, and histology revealed 22 PAs, 6 hyperplastic glands, and 3 parathyroid carcinomas (Supplemental Table 2). The locations of removed glands are listed in Supplemental Table 1.

All localizations described on PET/CT were concordant with surgery, except for 1 patient with a multiple endocrine neoplasia in which the uptake area was found in the lower left retropolar region on PET/CT whereas the PA was identified in the lower right retropolar region; 2 normal glands were also surgically removed on the left in this patient. In another patient with multiple foci observed on ^{18}F-FCH and ^{11}C-MET, pathologic tissue had probably been left in place because he was not cured after removal of 1 correctly localized lesion (parathyroid hyperplasia) and 2 thyroid nodules. One uptake area found on both PET/CT scans was not explored during surgery, and in 4 cases, parathyroid hyperplasia was found in false-negative ^{18}F-FCH PET/CT locations. On a per-lesion basis (Supplemental Table 2), sensitivity and positive predictive value were 84% and 90%, respectively, for ^{18}F-FCH PET/CT and 52% and 94%, respectively, for ^{11}C-MET PET/CT ($P < 0.0001$).

TABLE 2
Contingency Tables

Parameter	Positive ^{18}F-FCH	Negative ^{18}F-FCH	Total
Per patient			
Positive ^{11}C-MET	25	0	25
Negative ^{11}C-MET	14	14	28
Total	39	14	53
Per lesion			
Positive ^{11}C-MET	28	0	38
Negative ^{11}C-MET	19	18	37
Total	47	18	75

Contrast-to-Thyroid and PA Uptake Are Significantly Higher with ^{18}F-FCH PET/CT Than with ^{11}C-MET PET/CT

The visual comparison of the contrast-to-background in the detected anomalies for ^{18}F-FCH and ^{11}C-MET revealed a

superiority of ^{18}F-FCH over ^{11}C-MET, both at early and at late imaging times (Supplemental Fig. 3). Higher uptake was observed in 71%–82% (39–45/55) of anomalies for ^{18}F-FCH than for ^{11}C-MET, and a similar uptake of the 2 tracers was observed in 25% (14/55) and 16% (9/55) of cases for ^{18}F-FCH$_E$ and ^{18}F-FCH$_L$, respectively. When we consider only the cases that underwent parathyroidectomy, we found similar proportions. Only 1 case operated on had a lesion better visualized on ^{11}C-MET than on ^{18}F-FCH PET/CT.

Supplemental Figure 4 shows the distribution of SUV$_{max}$ PA and PA/thyroid for each tracer. SUV$_{max}$ PA on ^{18}F-FCH$_E$ and ^{18}F-FCH$_L$, given as median, was 3.26 (25th–75th percentiles, 2.45–4.74) and 3.52 (25th–75th percentiles, 2.58–4.91), respectively, whereas the median SUV$_{max}$ PA on ^{11}C-MET was 1.51 (25th–75th percentiles, 0.96–2.73). So, the SUV$_{max}$ PA on ^{18}F-FCH$_E$ and ^{18}F-FCH$_L$ was approximatively twice higher than ^{11}C-MET SUV$_{max}$ ($P < 0.0001$). There was no statistically significant difference between SUV$_{max}$ PA and PA/thyroid on ^{18}F-FCH$_E$ and ^{18}F-FCH$_L$ ($P = 0.3569$). PA/thyroid on ^{18}F-FCH$_E$ and ^{18}F-FCH$_L$ was 1.39 (25th–75th percentiles, 1.29–1.54) and 1.39 (25th–75th percentiles, 1.29–1.68), respectively ($P = 0.1005$). The quantitative analysis resulted in nonsignificant differences for both SUV$_{max}$ and PA/thyroid between adenoma and hyperplasia on both ^{18}F-FCH and ^{11}C-MET PET/CT.

We observed a positive correlation between PA/thyroid on ^{11}C-MET and ^{18}F-FCH PET/CT, despite the difference in the incorporation mechanisms (Fig. 2). Linear fit revealed that PA/thyroid was 11% higher in ^{18}F-FCH$_E$ and 31% higher in ^{18}F-FCH$_L$ than in ^{11}C-MET: for ^{18}F-FCH$_E$, $r = 0.6843$, with a slope of 1.11 and an intercept of 0.0175, and $r^2 = 0.79$; for ^{18}F-FCH$_L$, $r = 0.5665$, with a slope of 1.315 and an intercept of 0.046, and $r^2 = 0.75$.

DISCUSSION

To the best of our knowledge, this was the first study comparing ^{11}C-MET and ^{18}F-FCH tracers for the preoperative detection and localization of hyperfunctioning parathyroid tissue. Our results demonstrate the diagnostic superiority of ^{18}F-FCH over ^{11}C-MET PET/CT for PA and hyperplasia detection in patients with negative or inconclusive results on ^{99m}Tc-MIBI exploration.

Precise preoperative localization of a hyperfunctioning parathyroid gland is a prerequisite for efficient minimally invasive surgery. For this purpose, PET/CT recently emerged as a complementary second-line imaging technique with the advantage of a higher resolution associated with PET than with SPECT, as well as a shorter acquisition time (14).

Several publications concluded that the diagnostic performance of ^{18}F-FCH and ^{11}C-MET PET/CT for the localization of parathyroid lesions is better than that of conventional imaging methods ($3,7,8,11,15–17$). The present study confirmed the added value of this new tracer in the detection and precise localization of hyperfunctioning parathyroid tissue in the subgroup of patients with pHPT and negative or inconclusive results for ^{99m}Tc-MIBI with SPECT. The sensitivity of ^{18}F-FCH PET/CT was 96% on a per-patient basis and 84% on a per-lesion basis. As in the APACH1 study (8), we considered the histopathologic results as the gold standard for per-lesion analyses (8). Our findings are comparable to those reported in previous studies. A recent metaanalysis (18) concluded on pooled sensitivity of 93.7% and 91.3% on patient-based and lesion-based analyses, respectively. The detection rates of lesions were 77%–94% (on a patient basis) and 80%–96% (on a lesion basis) (15).

Our cohort included patients for whom the choice of surgical management was challenging (familial hyperparathyroidism, relapsing or persistent HPT, multiglandular forms) compared with most previous studies. Five of the 6 patients with persistent or relapsed postsurgical pHPT had areas of abnormal uptake revealed by ^{18}F-FCH, and we detected 19% of histologically confirmed multiglandular diseases. Still, most of our patients presented with a confirmed solitary lesion (81%), which was consistent with the rate reported in the literature (74% in Beheshti et al. (5)). There was no SUV$_{max}$ cutoff in ^{18}F-FCH that could be set to distinguish PA from parathyroid hyperplasia.

The optimal time point for ^{18}F-FCH image acquisition remains controversial ($3,17,19,20$). This controversy results from a 3-phase temporal pattern of ^{18}F-FCH PA uptake, with an early washout followed by an intermediate phase of stability and a late phase of increase (21). We therefore opted for a dual-time-point mode of acquisition in this study. On the basis of the visual evaluation of the images and the analysis of PA/thyroid, that is, a target-to-background ratio, we did not better discern lesions on the late images than on the early ones. Rep et al. (17) described in late-acquisition images a greater accumulation of ^{18}F-FCH in PA than in the thyroid, with a slightly slower decrease in signal, translating into a better lesion contrast. In agreement with our results, Broos et al. (19) reported a decrease in absolute uptake in PA over time, with an increase in contrast relative to the thyroid because of a weaker retention in the thyroid. Conversely, Michaud et al. (16) concluded that late images did not yield additional findings over early ones. Noticeably, in all previous studies, early images were acquired at 5 min after injection, whereas we decided for a slightly later acquisition. We found 2 patients with lesions showing a rapid ^{18}F-FCH washout in our population. Nevertheless, since most parathyroid lesions were observed on both acquisitions, we recommend performing the acquisition at 15 min, reserving additional late imaging for patients whose early acquisition has negative or inconclusive results, as also suggested by Uslu-Besli (22).

Before ^{18}F-FCH, ^{11}C-MET has been widely used as a reliable second-line agent in pHPT. Overall, in our study, ^{18}F-FCH showed a significantly higher sensitivity, with more cases diagnosed and higher accuracy than for ^{11}C-MET. The advantage of ^{18}F-FCH imaging
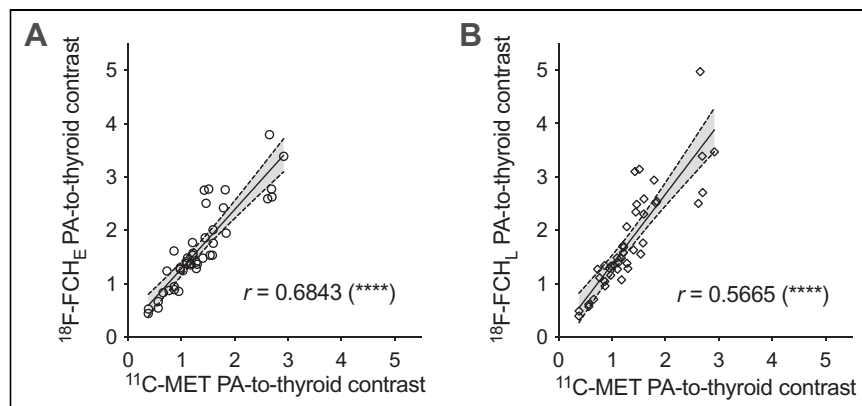

FIGURE 2. Correlation between ^{18}F-FCH (early [A] and late [B]) and ^{11}C-MET uptake. ****$P < 0.0001$.
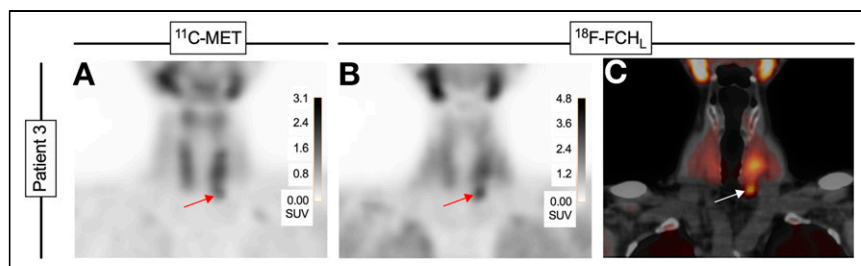
FIGURE 3. Patient 3. Coronal PET/CT images of 67-y-old woman with pHPT and inconclusive ^{99m}Tc-MIBI SPECT/CT (doubtful right inferior focus). (A) ^{11}C-MET images show asymmetric thyroid lobes with lower extension on left (arrow). (B) ^{18}F-FCH$_L$ images shows nodular uptake under base of left thyroid lobe (arrow). (C) PET/CT images detail nodular aspect of ^{18}F-FCH uptake (arrow) in PA confirmed at histopathologic analysis.

over ^{11}C-MET imaging seems to be strongly related to the fact that it produces more conclusive data. Indeed, 13 anomalies judged inconclusive on ^{11}C-MET PET/CT were considered positive on ^{18}F-FCH PET/CT. The superior imaging qualities of ^{18}F-labeled radiotracers over ^{11}C-labeled ones probably contribute to this better performance of ^{18}F-FCH. Apart from an effect of the positron energy, differences in the molecular properties and uptake mechanisms involved probably explain the differences in diagnostic performance between ^{18}F-FCH and ^{11}C-MET. Indeed, the 2 tracers explore very different biochemical pathways. ^{11}C-MET uptake most probably depends on expression and activity of amino acid transporters such as L-type amino acid transporter 1 and secondarily on its incorporation in the protein prepro-PTH. So, ^{11}C-MET uptake may be closely dependent on the level of synthesis and release of PTH. In contrast, ^{18}F-FCH uptake enters chief cells—those responsible for PTH production—and oxyphilic cells of parathyroid tissue through a specific membrane transporter. After reaching the cytoplasm, ^{18}F-FCH accumulates in the mitochondria in relation to its positive charge, as is the case for ^{99m}Tc-MIBI. In the chief cells, ^{18}F-FCH is also phosphorylated by a choline-kinase, which is overexpressed in patients with pHPT, leading to a phosphorylated form—that is, phosphatidylcholine—incorporated into the cytoplasmic membrane. The fact that 2 different mechanisms favor ^{18}F-FCH incorporation into the PTH-producing cells may represent an advantage over the other tracers such as ^{11}C-MET and ^{99m}Tc-MIBI (23).

For the evaluation of patients with pHPT and negative or inconclusive ^{99m}Tc-MIBI SPECT results, a pooled sensitivity of 86% had been reported in a per patient-based analysis of ^{11}C-MET PET/CT (24). Two other metaanalyses reported sensitivity ranging from 69% to 81% and a detection rate per patient of 70% (6,9). In our population, we reached a slightly lower sensitivity (60%), probably related to a high prevalence of clinical statuses that negatively influence the outcome of presurgical localization imaging, that is, postsurgical recurrence and familiar forms of pHPT (12,15). The visual analysis more frequently resulted in inconclusive uptake on ^{11}C-MET than on ^{18}F-FCH PET/CT. Noticeably, as in other analyses (11), we assimilated inconclusive results to negative ones because we considered that such results would preclude valuable image-guided planning of a minimally invasive parathyroidectomy. Such a position is not adopted by all authors (8).

Our study had some limitations. First, it did not directly compare ^{18}F-FCH PET/CT with ^{99m}Tc-MIBI SPECT/CT. Such analyses have already been made, showing the far superiority of ^{18}F-FCH imaging (3,8,11,15–17). This comparison was not among the objectives of our study since we selected only patients with pHPT and negative or

inconclusive ^{99m}Tc-MIBI exploration. Consequently, our results cannot be extrapolated to patients with tertiary hyperparathyroidism and cannot determine to what extent ^{18}F-FCH should replace ^{99m}Tc-MIBI as first-line molecular imaging in pHPT. Also, not all patients underwent surgery after presurgical PET/CT. So, our findings on the diagnostic impact of ^{18}F-FCH PET/CT relate only to the 26 of 53 patients for whom histopathologic data were available.

Finally, although ^{18}F-FCH PET/CT shows good performance for hyperfunctioning parathyroid tissue localization, potential drawbacks must be considered before adopting this modality as the single presurgical imaging procedure in pHPT. As in previous studies (12), we observed false-positive and false-negative findings. The 3 false-positive results related to 1 case of localization discordance between PET/CT and surgery, 1 case of uptake in a normal parathyroid gland, and 1 case of uptake in a thyroid nodule. Even if all 3 cases are classified as false-positive because of the lack of histologic evidence of PA or parathyroid hyperplasia, 2 patients were not cured after surgery, leaving open the possibility that resection did not involve the lesions pointed out by ^{18}F-FCH PET/CT. Five false-negative results concerned 4 cases of parathyroid hyperplasia and 1 patient with recurrent pHPT who ultimately had a PA resection during an extensive bilateral neck exploration. As in previous studies (11,14,16), discordant PET/CT interpretation between readers occurred in 2 situations in which nodular uptake was found within the thyroid gland. The differential diagnosis between a hypermetabolic thyroid nodule and an intrathyroidal PA appeared difficult because of the lack of comparison with a specific thyroid tracer (14). Still, as illustrated in Figure 3 and Supplemental Figure 2, mild to moderate physiologic ^{18}F-FCH uptake by the thyroid did not affect image interpretation in most of our cases, contrary to what has been reported (5). Another source of potential misinterpretation (Supplemental Table 3) is the presence of reactive lymph nodes in classic locations for PAs. Globally, despite the high prevalence of nodular thyroid in our patients and the frequent occurrence of hypermetabolic lymph nodes, both ^{18}F-FCH and ^{11}C-MET PET/CT correctly localized the parathyroid lesions in most surgically treated patients.

To determine which PET tracer should be privileged for a particular indication, various factors must be considered, including availability, diagnostic performance, and duration of examination (25). ^{18}F-FCH outperforms ^{11}C-MET for these 3 criteria.

CONCLUSION

Our study demonstrated that in the presence of biochemical evidence of pHPT with negative or inconclusive ^{99m}Tc-MIBI results, ^{18}F-FCH PET/CT performs better than ^{11}C-MET PET/CT for the detection of pathologic parathyroid tissue, allowing localization of PA or hyperplasia in 96% of patients. Since ^{18}F-FCH has been proved to be superior to ^{99m}Tc-MIBI in previous studies, our results position ^{18}F-FCH PET/CT as the modality of choice for lesion localization in pHPT.

DISCLOSURE

KEY POINTS

QUESTION: Is ^{18}F-FCH superior to ^{11}C-MET PET/CT for the localization of hyperfunctioning parathyroid tissue in patients with pHPT and negative or inconclusive ^{99m}Tc-MIBI SPECT findings?

PERTINENT FINDINGS: In this prospective clinical study, ^{18}F-FCH correctly localized lesions in 92% of patients, compared with 58% by ^{11}C-MET.

IMPLICATIONS FOR PATIENT CARE: ^{18}F-FCH is more sensitive than ^{11}C-MET for the localization of hyperfunctioning parathyroid tissue in patients with pHPT and negative or inconclusive ^{99m}Tc-MIBI SPECT results.

REFERENCES

1. Hindié E, Zanotti-Fregonara P, Tabarin A, et al. The role of radionuclide imaging in the surgical management of primary hyperparathyroidism. *J Nucl Med.* 2015;56: 737–744.

2. Bilezikian JP, Brandi ML, Eastell R, et al. Guidelines for the management of asymptomatic primary hyperparathyroidism: summary statement from the fourth international workshop. *J Clin Endocrinol Metab.* 2014;99:3561–3569.

3. Lezaic L, Rep S, Sever MJ, Kocjan T, Hocevar M, Fettich J. ^{18}F-fluorocholine PET/CT for localization of hyperfunctioning parathyroid tissue in primary hyperparathyroidism: a pilot study. *Eur J Nucl Med Mol Imaging.* 2014;41:2083–2089.

4. Treglia G, Sadeghi R, Schalin-Jäntti C, et al. Detection rate of ^{99m}Tc-MIBI single photon emission computed tomography (SPECT)/CT in preoperative planning for patients with primary hyperparathyroidism: a meta-analysis. *Head Neck.* 2016;38(suppl 1):E2159–E2172.

5. Beheshti M, Hehenwarter L, Paymani Z, et al. ^{18}F-fluorocholine PET/CT in the assessment of primary hyperparathyroidism compared with ^{99m}Tc-MIBI or ^{99m}Tc-tetrofosmin SPECT/CT: a prospective dual-centre study in 100 patients. *Eur J Nucl Med Mol Imaging.* 2018;45:1762–1771.

6. Kluijfhout WP, Pasternak JD, Drake FT, et al. Use of PET tracers for parathyroid localization: a systematic review and meta-analysis. *Langenbecks Arch Surg.* 2016; 401:925–935.

7. Tang B-N-T, Moreno-Reyes R, Blocklet D, et al. Accurate pre-operative localization of pathological parathyroid glands using ^{11}C-methionine PET/CT. *Contrast Media Mol Imaging.* 2008;3:157–163.

8. Quak E, Blanchard D, Houdu B, et al. F18-choline PET/CT guided surgery in primary hyperparathyroidism when ultrasound and MIBI SPECT/CT are negative or inconclusive: the APACH1 study. *Eur J Nucl Med Mol Imaging.* 2018; 45:658–666.

9. Caldarella C, Treglia G, Isgrò MA, Giordano A. Diagnostic performance of positron emission tomography using ^{11}C-methionine in patients with suspected parathyroid adenoma: a meta-analysis. *Endocrine.* 2013;43:78–83.

10. Quak E, Lheureux S, Reznik Y, Bardet S, Aide N. F18-choline, a novel PET tracer for parathyroid adenoma? *J Clin Endocrinol Metab.* 2013;98:3111–3112.

11. Michaud L, Burgess A, Huchet V, et al. Is ^{18}F-fluorocholine-positron emission tomography/computerized tomography a new imaging tool for detecting hyperfunctioning parathyroid glands in primary or secondary hyperparathyroidism? *J Clin Endocrinol Metab.* 2014;99:4531–4536.

12. Grimaldi S, Young J, Kamenicky P, et al. Challenging pre-surgical localization of hyperfunctioning parathyroid glands in primary hyperparathyroidism: the added value of ^{18}F-fluorocholine PET/CT. *Eur J Nucl Med Mol Imaging.* 2018;45:1772–1780.

13. Otabashi M, Desfours C, Vergote T, Brichard L, Morelle J-L, Philippart G. Automated production of high purity [^{18}F]fluorocholine at high activity on the AllInOne Synthesizer [abstract]. *J Nucl Med.* 2016;57(suppl 2):2732.

14. Imperiale A, Taïeb D, Hindié E. ^{18}F-fluorocholine PET/CT as a second line nuclear imaging technique before surgery for primary hyperparathyroidism. *Eur J Nucl Med Mol Imaging.* 2018;45:654–657.

15. Kluijfhout WP, Vorselaars WMCM, van den Berk SAM, et al. Fluorine-18 fluorocholine PET-CT localizes hyperparathyroidism in patients with inconclusive conventional imaging: a multicenter study from The Netherlands. *Nucl Med Commun.* 2016;37:1246–1252.

16. Michaud L, Balogova S, Burgess A, et al. A pilot comparison of ^{18}F-fluorocholine PET/CT, ultrasonography and ^{123}I/^{99m}Tc-sestaMIBI dual-phase dual-isotope scintigraphy in the preoperative localization of hyperfunctioning parathyroid glands in primary or secondary hyperparathyroidism: influence of thyroid anomalies. *Medicine (Baltimore).* 2015;94:e1701.

17. Rep S, Lezaic L, Kocjan T, et al. Optimal scan time for evaluation of parathyroid adenoma with [^{18}F]-fluorocholine PET/CT. *Radiol Oncol.* 2015;49:327–333.

18. Evangelista L, Ravelli I, Magnani F, et al. ^{18}F-choline PET/CT and PET/MRI in primary and recurrent hyperparathyroidism: a systematic review of the literature. *Ann Nucl Med.* 2020;34:601–619.

19. Broos WA, Wondergem M, van der Zant F, Knol R. Dual-time-point ^{18}F-fluorocholine PET/CT in parathyroid imaging. *J Nucl Med.* 2019;60:1605–1610.

20. Jun G, Pampaloni MH, Villanueva-Meyer J, Ravanfar V, Suh I, Hope T. 18-F-fluorocholine PETMR: optimizing injection delay for parathyroid adenoma localization [abstract]. *J Nucl Med.* 2018;59(suppl 1):236.

21. Morland D, Richard C, Godard F, Deguelte S, Delemer B. Temporal uptake patterns of ^{18}F-fluorocholine among hyperfunctioning parathyroid glands. *Clin Nucl Med.* 2018;43:504–505.

22. Uslu-Beşli L, Sonmezoglu K, Teksoz S, et al. Performance of F-18 fluorocholine PET/CT for detection of hyperfunctioning parathyroid tissue in patients with elevated parathyroid hormone levels and negative or discrepant results in conventional imaging. *Korean J Radiol.* 2020;21:236–247.

23. Ferrari C, Santo G, Mammucci P, Pisani AR, Sardaro A, Rubini G. Diagnostic value of choline PET in the preoperative localization of hyperfunctioning parathyroid gland(s): a comprehensive overview. *Biomedicines.* 2021;9:231.

24. Yuan L, Liu J, Kan Y, Yang J, Wang X. The diagnostic value of ^{11}C-methionine PET in hyperparathyroidism with negative ^{99m}Tc-MIBI SPECT: a meta-analysis. *Acta Radiol.* 2017;58:558–564.

25. Giovanella L, Bacigalupo L, Treglia G, Piccardo A. Will ^{18}F-fluorocholine PET/CT replace other methods of preoperative parathyroid imaging? *Endocrine.* 2021; 71:285–297.